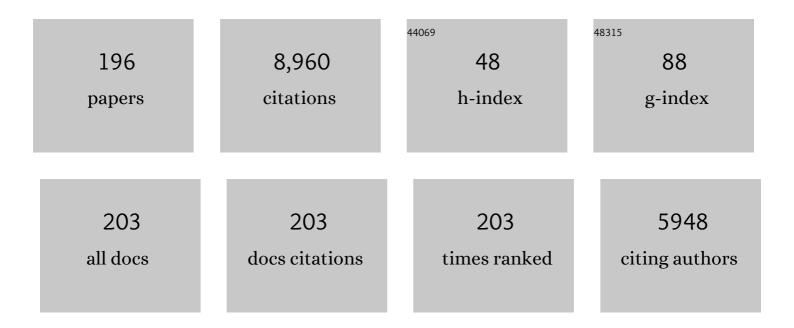
List of Publications by Year in descending order

Source: https://exaly.com/author-pdf/1110265/publications.pdf Version: 2024-02-01



#	Article	IF	CITATIONS
1	<i>In vivo</i> multiphoton microscopy of NADH and FAD redox states, fluorescence lifetimes, and cellular morphology in precancerous epithelia. Proceedings of the National Academy of Sciences of the United States of America, 2007, 104, 19494-19499.	7.1	898
2	Fluorescence Spectroscopy of Neoplastic and Non-Neoplastic Tissues. Neoplasia, 2000, 2, 89-117.	5.3	572
3	Metabolic Mapping of MCF10A Human Breast Cells via Multiphoton Fluorescence Lifetime Imaging of the Coenzyme NADH. Cancer Research, 2005, 65, 8766-8773.	0.9	351
4	In vivo multiphoton fluorescence lifetime imaging of protein-bound and free nicotinamide adenine dinucleotide in normal and precancerous epithelia. Journal of Biomedical Optics, 2007, 12, 024014.	2.6	317
5	Monte Carlo-based inverse model for calculating tissue optical properties Part I: Theory and validation on synthetic phantoms. Applied Optics, 2006, 45, 1062.	2.1	276
6	In vivo diagnosis of cervical intraepithelial neoplasia using 337-nm-excited laser-induced fluorescence Proceedings of the National Academy of Sciences of the United States of America, 1994, 91, 10193-10197.	7.1	269
7	Phase measurement of light absorption and scatter in human tissue. Review of Scientific Instruments, 1998, 69, 3457-3481.	1.3	238
8	Cervical Precancer Detection Using a Multivariate Statistical Algorithm Based on Laserâ€Induced Fluorescence Spectra at Multiple Excitation Wavelengths. Photochemistry and Photobiology, 1996, 64, 720-735.	2.5	231
9	Multiphoton Microscopy of Endogenous Fluorescence Differentiates Normal, Precancerous, and Cancerous Squamous Epithelial Tissues. Cancer Research, 2005, 65, 1180-1186.	0.9	214
10	Development of a Fiber Optic Probe to Measure NIR Raman Spectra of Cervical Tissue In Vivo. Photochemistry and Photobiology, 1998, 68, 427-431.	2.5	161
11	Optical Redox Ratio Differentiates Breast Cancer Cell Lines Based on Estrogen Receptor Status. Cancer Research, 2010, 70, 4759-4766.	0.9	158
12	Fluorescence Spectroscopy: A Diagnostic Tool for Cervical Intraepithelial Neoplasia (CIN). Gynecologic Oncology, 1994, 52, 31-38.	1.4	155
13	Quantitative Optical Spectroscopy: A Robust Tool for Direct Measurement of Breast Cancer Vascular Oxygenation and Total Hemoglobin Content <i>In vivo</i> . Cancer Research, 2009, 69, 2919-2926.	0.9	154
14	Advances in quantitative UV–visible spectroscopy for clinical and pre-clinical application in cancer. Current Opinion in Biotechnology, 2009, 20, 119-131.	6.6	125
15	Comparison of multiexcitation fluorescence and diffuse reflectance spectroscopy for the diagnosis of breast cancer (march 2003). IEEE Transactions on Biomedical Engineering, 2003, 50, 1233-1242.	4.2	121
16	Development of a multivariate statistical algorithm to analyze human cervical tissue fluorescence spectra acquired in vivo. , 1996, 19, 46-62.		120
17	Development of a Fiber Optic Probe to Measure NIR Raman Spectra of Cervical Tissue In Vivo. Photochemistry and Photobiology, 1998, 68, 427.	2.5	118
18	Monte Carlo-based inverse model for calculating tissue optical properties Part II: Application to breast cancer diagnosis. Applied Optics, 2006, 45, 1072.	2.1	116

#	Article	IF	CITATIONS
19	Spectroscopic diagnosis of cervical intraepithelial neoplasia (CIN) in vivo using laser-induced fluorescence spectra at multiple excitation wavlengths. , 1996, 19, 63-74.		113
20	Trans-abdominal monitoring of fetal arterial blood oxygenation using pulse oximetry. Journal of Biomedical Optics, 2000, 5, 391.	2.6	99
21	Diagnosis of breast cancer using diffuse reflectance spectroscopy: Comparison of a Monte Carlo versus partial least squares analysis based feature extraction technique. Lasers in Surgery and Medicine, 2006, 38, 714-724.	2.1	97
22	Autofluorescence and diffuse reflectance properties of malignant and benign breast tissues. Annals of Surgical Oncology, 2004, 11, 65-70.	1.5	85
23	Relation between fluorescence spectra of dilute and turbid samples. Applied Optics, 1994, 33, 414.	2.1	84
24	Low Temperature Fluorescence Imaging of Freeze-trapped Human Cervical Tissues. Optics Express, 2001, 8, 335.	3.4	84
25	Effect of fiber optic probe geometry on depth-resolved fluorescence measurements from epithelial tissues: a Monte Carlo simulation. Journal of Biomedical Optics, 2003, 8, 237.	2.6	84
26	Experimental validation of Monte Carlo modeling of fluorescence in tissues in the UV-visible spectrum. Journal of Biomedical Optics, 2003, 8, 223.	2.6	83
27	Quantitative Physiology of the Precancerous Cervix In Vivo through Optical Spectroscopy. Neoplasia, 2009, 11, 325-332.	5.3	80
28	Chromophore based analyses of steadyâ€state diffuse reflectance spectroscopy: current status and perspectives for clinical adoption. Journal of Biophotonics, 2015, 8, 9-24.	2.3	79
29	Ensembles of radial basis function networks for spectroscopic detection of cervical precancer. IEEE Transactions on Biomedical Engineering, 1998, 45, 953-961.	4.2	78
30	Fluorescence spectroscopy for diagnosis of squamous intraepithelial lesions of the cervix. Obstetrics and Gynecology, 1999, 93, 462-470.	2.4	76
31	Autofluorescence Spectroscopy of Normal and Malignant Human Breast Cell Lines¶. Photochemistry and Photobiology, 2003, 78, 462.	2.5	75
32	Rapid noninvasive optical imaging of tissue composition in breast tumor margins. American Journal of Surgery, 2009, 198, 566-574.	1.8	73
33	Diagnosis of breast cancer using fluorescence and diffuse reflectance spectroscopy: a Monte-Carlo-model-based approach. Journal of Biomedical Optics, 2008, 13, 034015.	2.6	72
34	Multiphoton Redox Ratio Imaging for Metabolic Monitoring In Vivo. Methods in Molecular Biology, 2010, 594, 155-162.	0.9	71
35	Sequential estimation of optical properties of a two-layered epithelial tissue model from depth-resolved ultraviolet-visible diffuse reflectance spectra. Applied Optics, 2006, 45, 4776.	2.1	70
36	Optimal methods for fluorescence and diffuse reflectance measurements of tissue biopsy samples. Lasers in Surgery and Medicine, 2002, 30, 191-200.	2.1	69

#	Article	IF	CITATIONS
37	Development of Algorithms for Automated Detection of Cervical Pre-Cancers With a Low-Cost, Point-of-Care, Pocket Colposcope. IEEE Transactions on Biomedical Engineering, 2019, 66, 2306-2318.	4.2	69
38	Relationship between depth of a target in a turbid medium and fluorescence measured by a variable-aperture method. Optics Letters, 2002, 27, 104.	3.3	66
39	Investigation of fiber-optic probe designs for optical spectroscopic diagnosis of epithelial pre-cancers. Lasers in Surgery and Medicine, 2004, 34, 25-38.	2.1	65
40	A Robust Monte Carlo Model for the Extraction of Biological Absorption and Scattering <i>In Vivo</i> . IEEE Transactions on Biomedical Engineering, 2009, 56, 960-968.	4.2	65
41	Performance metrics of an optical spectral imaging system for intra-operative assessment of breast tumor margins. Optics Express, 2010, 18, 8058.	3.4	64
42	Scaling method for fast Monte Carlo simulation of diffuse reflectance spectra from multilayered turbid media. Journal of the Optical Society of America A: Optics and Image Science, and Vision, 2007, 24, 1011.	1.5	63
43	Optical Assesssment of Tumor Resection Margins in the Breast. IEEE Journal of Selected Topics in Quantum Electronics, 2010, 16, 530-544.	2.9	60
44	Optical breast cancer margin assessment: an observational study of the effects of tissue heterogeneity on optical contrast. Breast Cancer Research, 2010, 12, R91.	5.0	59
45	Using Optical Spectroscopy to Longitudinally Monitor Physiological Changes within Solid Tumors. Neoplasia, 2009, 11, 889-900.	5.3	57
46	Uptake of 2-NBDG as a method to monitor therapy response in breast cancer cell lines. Breast Cancer Research and Treatment, 2011, 126, 55-62.	2.5	56
47	Design of a Novel Low Cost Point of Care Tampon (POCkeT) Colposcope for Use in Resource Limited Settings. PLoS ONE, 2015, 10, e0135869.	2.5	55
48	Portable, Fiber-Based, Diffuse Reflection Spectroscopy (DRS) Systems for Estimating Tissue Optical Properties. Applied Spectroscopy, 2011, 65, 206-215.	2.2	54
49	Quantitative optical spectroscopy can identify long-term local tumor control in irradiated murine head and neck xenografts. Journal of Biomedical Optics, 2009, 14, 054051.	2.6	53
50	Use of a multiseparation fiber optic probe for the optical diagnosis of breast cancer. Journal of Biomedical Optics, 2005, 10, 024032.	2.6	52
51	Monte-Carlo-based model for the extraction of intrinsic fluorescence from turbid media. Journal of Biomedical Optics, 2008, 13, 024017.	2.6	52
52	Experimental proof of the feasibility of using an angled fiber-optic probe for depth-sensitive fluorescence spectroscopy of turbid media. Optics Letters, 2004, 29, 2034.	3.3	50
53	Radiation induces aerobic glycolysis through reactive oxygen species. Radiotherapy and Oncology, 2013, 106, 390-396.	0.6	48
54	Resonance Raman Spectroscopy at 257 nm Excitation of Normal and Malignant Cultured Breast and Cervical Cells. Applied Spectroscopy, 1999, 53, 82-85.	2.2	45

#	Article	IF	CITATIONS
55	Comparison of a physical model and principal component analysis for the diagnosis of epithelial neoplasias in vivo using diffuse reflectance spectroscopy. Optics Express, 2007, 15, 7863.	3.4	45
56	Optical and Radioiodinated Tethered Hsp90 Inhibitors Reveal Selective Internalization of Ectopic Hsp90 in Malignant Breast Tumor Cells. Chemistry and Biology, 2013, 20, 1187-1197.	6.0	43
57	FLUORESCENCE SPECTROSCOPY FOR DIAGNOSIS OF SQUAMOUS INTRAEPITHELIAL LESIONS OF THE CERVIX. Obstetrics and Gynecology, 1999, 93, 462-470.	2.4	42
58	Quantitative diffuse reflectance and fluorescence spectroscopy: tool to monitor tumor physiology in vivo. Journal of Biomedical Optics, 2009, 14, 024010.	2.6	42
59	High-resolution three-dimensional scanning optical image system for intrinsic and extrinsic contrast agents in tissue. Review of Scientific Instruments, 2002, 73, 172-178.	1.3	40
60	Photon migration through fetal head in utero using continuous wave, near infrared spectroscopy: clinical and experimental model studies. Journal of Biomedical Optics, 2000, 5, 173.	2.6	38
61	Transabdominal near infrared oximetry of hypoxic stress in fetal sheep brain in utero. Proceedings of the United States of America, 2003, 100, 12950-12954.	7.1	38
62	Cost-effective diffuse reflectance spectroscopy device for quantifying tissue absorption and scattering in vivo. Journal of Biomedical Optics, 2008, 13, 060505.	2.6	38
63	Noninvasive monitoring of tissue hemoglobin using UV-VIS diffuse reflectance spectroscopy: a pilot study. Optics Express, 2009, 17, 23396.	3.4	37
64	Fast and noninvasive fluorescence imaging of biological tissues in vivo using a flying-spot scanner. IEEE Transactions on Biomedical Engineering, 2001, 48, 1034-1041.	4.2	36
65	Preferential accumulation of 5-aminolevulinic acid-induced protoporphyrin IX in breast cancer: a comprehensive study on six breast cell lines with varying phenotypes. Journal of Biomedical Optics, 2010, 15, 018002.	2.6	36
66	Development of enhanced ethanol ablation as an alternative to surgery in treatment of superficial solid tumors. Scientific Reports, 2017, 7, 8750.	3.3	35
67	A strategy for quantitative spectral imaging of tissue absorption and scattering using light emitting diodes and photodiodes. Optics Express, 2009, 17, 1372.	3.4	33
68	Optical Spectral Surveillance of Breast Tissue Landscapes for Detection of Residual Disease in Breast Tumor Margins. PLoS ONE, 2013, 8, e69906.	2.5	33
69	Design and preliminary analysis of a vaginal inserter for speculum-free cervical cancer screening. PLoS ONE, 2017, 12, e0177782.	2.5	32
70	Near-simultaneous intravital microscopy of glucose uptake and mitochondrial membrane potential, key endpoints that reflect major metabolic axes in cancer. Scientific Reports, 2017, 7, 13772.	3.3	30
71	Optimization of a Widefield Structured Illumination Microscope for Non-Destructive Assessment and Quantification of Nuclear Features in Tumor Margins of a Primary Mouse Model of Sarcoma. PLoS ONE, 2013, 8, e68868.	2.5	30
72	Photon migration through fetal head <italic>in utero</italic> using continuous wave, near-infrared spectroscopy: development and evaluation of experimental and numerical models. Journal of Biomedical Optics, 2000, 5, 163.	2.6	29

#	Article	IF	CITATIONS
73	Model based and empirical spectral analysis for the diagnosis of breast cancer. Optics Express, 2008, 16, 14961.	3.4	27
74	Advancing Optical Imaging for Breast Margin Assessment: An Analysis of Excisional Time, Cautery, and Patent Blue Dye on Underlying Sources of Contrast. PLoS ONE, 2012, 7, e51418.	2.5	27
75	Delivery Rate Affects Uptake of a Fluorescent Clucose Analog in Murine Metastatic Breast Cancer. PLoS ONE, 2013, 8, e76524.	2.5	27
76	An integrated strategy for improving contrast, durability, and portability of a Pocket Colposcope for cervical cancer screening and diagnosis. PLoS ONE, 2018, 13, e0192530.	2.5	27
77	Fluorescence Spectroscopy: An Adjunct Diagnostic Tool to Image-Guided Core Needle Biopsy of the Breast. IEEE Transactions on Biomedical Engineering, 2009, 56, 2518-2528.	4.2	26
78	Instrument independent diffuse reflectance spectroscopy. Journal of Biomedical Optics, 2011, 16, 011010.	2.6	26
79	Sources of phase noise in homodyne and heterodyne phase modulation devices used for tissue oximetry studies. Review of Scientific Instruments, 1998, 69, 3042-3054.	1.3	25
80	Oxygen and Perfusion Kinetics in Response to Fractionated Radiation Therapy in FaDu Head and Neck Cancer Xenografts Are Related to Treatment Outcome. International Journal of Radiation Oncology Biology Physics, 2016, 96, 462-469.	0.8	25
81	Method to Determine Tissue Fluorescence Efficiency in vivo and Predict Signal-to-Noise Ratio for Spectrometers. Applied Spectroscopy, 1998, 52, 943-951.	2.2	24
82	Diffuse reflectance spectroscopy with a self-calibrating fiber optic probe. Optics Letters, 2008, 33, 1783.	3.3	24
83	Rapid staining and imaging of subnuclear features to differentiate between malignant and benign breast tissues at a point-of-care setting. Journal of Cancer Research and Clinical Oncology, 2016, 142, 1475-1486.	2.5	24
84	International Image Concordance Study to Compare a Point-of-Care Tampon Colposcope With a Standard-of-Care Colposcope. Journal of Lower Genital Tract Disease, 2017, 21, 112-119.	1.9	24
85	Non-Invasive, Simultaneous Quantification of Vascular Oxygenation and Glucose Uptake in Tissue. PLoS ONE, 2015, 10, e0117132.	2.5	24
86	Delivery-Corrected Imaging of Fluorescently-Labeled Glucose Reveals Distinct Metabolic Phenotypes in Murine Breast Cancer. PLoS ONE, 2014, 9, e115529.	2.5	23
87	A Quantitative Diffuse Reflectance Imaging (QDRI) System for Comprehensive Surveillance of the Morphological Landscape in Breast Tumor Margins. PLoS ONE, 2015, 10, e0127525.	2.5	23
88	Antepartum, transabdominal near infrared spectroscopy: Feasibility of measuring photon migration through the fetal head in utero. , 1999, 8, 275-288.		22
89	Visible light optical spectroscopy is sensitive to neovascularization in the dysplastic cervix. Journal of Biomedical Optics, 2010, 15, 057006.	2.6	22
90	A low-cost, portable, and quantitative spectral imaging system for application to biological tissues. Optics Express, 2010, 18, 12630.	3.4	22

#	Article	IF	CITATIONS
91	Effect of optical clearing agents on the in vivo optical properties of squamous epithelial tissue. Lasers in Surgery and Medicine, 2006, 38, 920-927.	2.1	21
92	Electromagnetic Spectroscopy of Normal Breast Tissue Specimens Obtained From Reduction Surgeries: Comparison of Optical and Microwave Properties. IEEE Transactions on Biomedical Engineering, 2008, 55, 2444-2451.	4.2	21
93	Metaboloptics: Visualization of the tumor functional landscape via metabolic and vascular imaging. Scientific Reports, 2018, 8, 4171.	3.3	21
94	Relationship Between Collagen Autofluorescence of the Human Cervix and Menopausal Status. Photochemistry and Photobiology, 2003, 77, 653.	2.5	20
95	Rapid ratiometric determination of hemoglobin concentration using UV-VIS diffuse reflectance at isosbestic wavelengths. Optics Express, 2010, 18, 18779.	3.4	20
96	A diffuse reflectance spectral imaging system for tumor margin assessment using custom annular photodiode arrays. Biomedical Optics Express, 2012, 3, 3211.	2.9	20
97	A Fluorescence-Guided Laser Ablation System for Removal of Residual Cancer in a Mouse Model of Soft Tissue Sarcoma. Theranostics, 2016, 6, 155-166.	10.0	20
98	Statistical techniques for diagnosing CIN using fluorescence spectroscopy: SVD and CART. Journal of Cellular Biochemistry, 1995, 59, 125-130.	2.6	19
99	Modeling photon transport in transabdominal fetal oximetry. Journal of Biomedical Optics, 2000, 5, 277.	2.6	19
100	Understanding Factors Governing Distribution Volume of Ethyl Cellulose-Ethanol to Optimize Ablative Therapy in the Liver. IEEE Transactions on Biomedical Engineering, 2020, 67, 2337-2348.	4.2	19
101	Towards a field-compatible optical Spectroscopic device for cervical cancer screening in resource-limited settings: effects of calibration and pressure. Optics Express, 2011, 19, 17908.	3.4	18
102	Optical Imaging of Glucose Uptake and Mitochondrial Membrane Potential to Characterize Her2 Breast Tumor Metabolic Phenotypes. Molecular Cancer Research, 2019, 17, 1545-1555.	3.4	18
103	Feasibility of near-infrared diffuse optical spectroscopy on patients undergoing imageguided core-needle biopsy. Optics Express, 2007, 15, 7335.	3.4	17
104	Quantitative Segmentation of Fluorescence Microscopy Images of Heterogeneous Tissue: Application to the Detection of Residual Disease in Tumor Margins. PLoS ONE, 2013, 8, e66198.	2.5	17
105	Measuring tumor cycling hypoxia and angiogenesis using a sideâ€firing fiber optic probe. Journal of Biophotonics, 2014, 7, 552-564.	2.3	16
106	In Vivo Optical Metabolic Imaging of Long-Chain Fatty Acid Uptake in Orthotopic Models of Triple-Negative Breast Cancer. Cancers, 2021, 13, 148.	3.7	16
107	Leveraging ectopic Hsp90 expression to assay the presence of tumor cells and aggressive tumor phenotypes in breast specimens. Scientific Reports, 2017, 7, 17487.	3.3	15
108	Diagnosis of Breast Cancer Using Optical Spectroscopy. Medical Laser Application: International Journal for Laser Treatment and Research, 2003, 18, 233-248.	0.3	14

#	Article	IF	CITATIONS
109	[21] Steady-state fluorescence imaging of neoplasia. Methods in Enzymology, 2003, 361, 452-481.	1.0	14
110	Rapid Determination of Oxygen Saturation and Vascularity for Cancer Detection. PLoS ONE, 2013, 8, e82977.	2.5	14
111	Experimental validation of an inverse fluorescence Monte Carlo model to extract concentrations of metabolically relevant fluorophores from turbid phantoms and a murine tumor model. Journal of Biomedical Optics, 2012, 17, 0780031.	2.6	13
112	Digital Health Strategies for Cervical Cancer Control in Low- and Middle-Income Countries: Systematic Review of Current Implementations and Gaps in Research. Journal of Medical Internet Research, 2021, 23, e23350.	4.3	13
113	Micro-anatomical quantitative optical imaging: toward automated assessment of breast tissues. Breast Cancer Research, 2015, 17, 105.	5.0	12
114	Algorithms for differentiating between images of heterogeneous tissue across fluorescence microscopes. Biomedical Optics Express, 2016, 7, 3412.	2.9	12
115	Near-simultaneous quantification of glucose uptake, mitochondrial membrane potential, and vascular parameters in murine flank tumors using quantitative diffuse reflectance and fluorescence spectroscopy. Biomedical Optics Express, 2018, 9, 3399.	2.9	12
116	Monte Carlo-based inverse model for calculating tissue optical properties Part I: Theory and validation on synthetic phantoms: erratum. Applied Optics, 2007, 46, 6847.	2.1	11
117	Assessment of the sensitivity and specificity of tissue-specific-based and anatomical-based optical biomarkers for rapid detection of human head and neck squamous cell carcinoma. Oral Oncology, 2014, 50, 848-856.	1.5	11
118	Exploiting heat shock protein expression to develop a non-invasive diagnostic tool for breast cancer. Scientific Reports, 2019, 9, 3461.	3.3	11
119	Polymer-assisted intratumoral delivery of ethanol: Preclinical investigation of safety and efficacy in a murine breast cancer model. PLoS ONE, 2021, 16, e0234535.	2.5	11
120	Development of a multivariate statistical algorithm to analyze human cervical tissue fluorescence spectra acquired in vivo. Lasers in Surgery and Medicine, 1996, 19, 46-62.	2.1	11
121	Endoscopically compatible near-infrared photon migration probe. Optics Letters, 2004, 29, 2022.	3.3	10
122	Miniature spectral imaging device for wide-field quantitative functional imaging of the morphological landscape of breast tumor margins. Journal of Biomedical Optics, 2017, 22, 026007.	2.6	10
123	A novel speculum-free imaging strategy for visualization of the internal female lower reproductive system. Scientific Reports, 2020, 10, 16570.	3.3	10
124	Wavelength Optimization for Quantitative Spectral Imaging of Breast Tumor Margins. PLoS ONE, 2013, 8, e61767.	2.5	10
125	Detection of Squamous Cell Carcinoma and Corresponding Biomarkers Using Optical Spectroscopy. Otolaryngology - Head and Neck Surgery, 2011, 144, 390-394.	1.9	9
126	A quantitative microscopic approach to predict local recurrence based on <i>in vivo</i> in traoperative imaging of sarcoma tumor margins. International Journal of Cancer, 2015, 137, 2403-2412.	5.1	8

127 Simultaneous in two optical quantification of key metabolic and vascular endpoints reveals tumor metabolic dwerthy in murine breast tumor medds. Journal of Biophotonics, 2019, 12, e201800372. 2.3 8 128 Multinally investive ethyl cellulose ethanol abletion in domesticated cats with naturally occurring 1.8 8 129 Use of Cenetic Algorithms to Opticar Polic Polic Polic Debegin for the Extraction of Issue Optical 4.2 7 130 Structured Illumination Microscopy and a Quantitative Image Analysis for the Detection of Positive Margins in a Pre-Clinical Cenetically Engineering, 2007, 54, 1534-1535. 4.2 7 130 Structured Illumination Microscopy and a Quantitative Image Analysis for the Detection of Positive Pre-Clinical Cenetically Engineering 2007, 54, 1534-1535. 4.2 7 131 Correlation of branet it issue biologing and optical gianutures to improve margin assessment techning ablation of cenvical dysplasia. Scientific 0.9 7 132 Distinct Angiogenic Changes during Caringegnesis Defined by Nevel Label-Free Dark-Field Imaging in a Reports, 2021, 11, 16869. 0.3 7 133 Reports, 2021, 11, 16869. 0.3 7 0.3 7 134 Rediologic pathologic analysis of increased ethanol localization and ablative extent achieved by ethyl 3.3 7 134 Rediologic pathologic analysis of incre	#	Article	IF	CITATIONS
124 head and neck cancers: Six cats. Veterinary and Comparative Oncology, 2021, 19, 492-500. 1.5 5 129 Use of Genetic Algorithms to Optimize Fiber Optic Probe Design for the Extraction of Tissue Optical 4.2 7 130 Structured Illumination Microscopy and a Quantitative Image Analysis for the Detection of Positive 2.5 7 131 Correlation of breast tissue histology and optical signatures to Improve margin assessment 2.6 7 132 Distinct Angiogenic Changes during Carcinogenesis Defined by Novel Label-Free Dark-Field Imaging in a 0.9 7 133 Optimizinging ethyl cellulose ethanol delivery towards enabling ablation of cervical dysplasia. Scientific 8.3 7 134 Rediologic-pathologic analysis of increased ethanol localization and ablative extent achieved by ethyl 8.3 7 135 Accompact, cost-effective diffuse reflectance spectroscopic imaging system for quantitative tissue 0.8 6 136 carchied optical imaging reveals vascular changes in an inductibe hamster cheek pouch model cluring 2.9 6 137 cambridgenesis. Biomedical Optics Express, 2015, 71, 2027. 32/07, 2027. 3 6 138 Rediologic-pathologic analysis of increased ethanol localization and ablative extent achieved by ethyl 8.3	127		2.3	8
129 Properties, IEEE Transactions on Biomedical Engineering, 2007, 54, 1533-1535. 4.2 7 130 Structured Illumination Microscopy and a Quantitative Image Analysis for the Detection of Positive Margins in a Pre-Clinical Cenetically Engineered Mouse Model of Sarcoma, PLoS ONE, 2016, 11, e0147006. 2.5 7 131 Correlation of breast tissue histology and optical signatures to improve margin assessment. 2.6 7 132 Distinct Anglogenic Changes during Carcinogenesis Defined by Novel Label-Free Dark-Field Imaging in a 0.9 7 133 Optimizingio, ethyl collulose ethanol delivery towards enabling ablation of cervical dysplasia. Scientific Reports, 2021, 11, 16869. 3.3 7 134 Radiologic-pathologic analysis of increased ethanol localization and ablative extent achieved by ethyl cellulose ethanol delivery towards enabling ablation of cervical dysplasia. Scientific Reports, 2021, 11, 20700. 3.3 7 135 Accmpact, cost-effective diffuse reflectance spectroscopic Imaging system for quantitative tissue absorption and scattering. Proceedings of SPIE, 2011, 0.8 6 136 Dark field optical imaging reveals vascular changes in an inducible hamster cheek pouch model during cancers with a low-cost point-of-care Packet colposcope, 2020, 2020, 1148-1151. 6 137 Combining multiple contrasts for improving machine learning-based classification of cervical disproscope for Surgery in Low- and Middle-Income C	128	Minimally invasive ethyl cellulose ethanol ablation in domesticated cats with naturally occurring head and neck cancers: Six cats. Veterinary and Comparative Oncology, 2021, 19, 492-500.	1.8	8
Margins in a Pre-Clinical Genetically Engineered Mouse Model of Sarcoma. PLoS ONE, 2016, 11, e0147006. 2.0 7 131 Correlation of breast tissue histology and optical signatures to improve margin assessment 2.6 7 132 Distinct Angiogenic Changes during Carcinogenesis Defined by Novel Label-Free Dark-Field Imaging in a 0.9 7 133 Optimizingio, ethyl cellulose-ethanol delivery towards enabling ablation of cervical dysplasia. Scientific 3.3 7 134 Redologic pathologic analysis of increased ethanol localization and ablative extent achieved by ethyl 3.3 7 135 A compact, cost-effective diffuse reflectance spectroscopic imaging system for quantitative tissue 0.8 6 136 Dark field optical imaging reveals vascular changes in an inducible hamster cheek pouch model during 2.9 6 137 Combining multiple contrasts for improving machine learning-based classification of cervical 0.8 6 138 Quantitative spectral reflectance imaging device for intraoperative breast tumor margin assessment. 5 5 139 An Accessible Laparoscope for Surgery in Low- and Middle- Income Countries. Annals of Biomedical 2.5 6 139 An Accessible Laparoscope for Surgery in Low- and Middle- Income Countries. Annals of Biomedical 2.5 5	129		4.2	7
111 techniques. Journal of Biomedical Optics. 2016, 21, 066014. 2-30 7 132 Distinct Angiogenic Changes during Carcinogenesis Defined by Novel Label-Free Dark-Field Imaging in a 0.9 7 133 Reports, 2021, 11, 16869. 3.3 7 134 Radiologic-pathologic analysis of increased ethanol localization and ablative extent achieved by ethyl 3.3 7 134 Radiologic-pathologic analysis of increased ethanol localization and ablative extent achieved by ethyl 3.3 7 135 Acompact, cost-effective diffuse reflectance spectroscopic imaging system for quantitative tissue 0.8 6 136 Dark field optical imaging reveals vascular changes in an inducible hamster cheek pouch model during 2.9 6 137 Combining multiple contrasts for improving machine learning-based classification of cervical 6 6 138 Quantitative spectral reflectance imaging device for Intraoperative breast tumor margin assessment. , 5 5 139 An Accessible Laparoscope for Surgery in Low- and Middle-Income Countries. Annals of Biomedical 2.5 5 140 Autofluorescence Spectroscopy of Normal and Malignant Human Breast Cell LinesAf, Photochemistry 2.5 4 141 Custom annular photodetector arrays for	130	Structured Illumination Microscopy and a Quantitative Image Analysis for the Detection of Positive Margins in a Pre-Clinical Genetically Engineered Mouse Model of Sarcoma. PLoS ONE, 2016, 11, e0147006.	2.5	7
Hamster Cheek Pouch Model. Cancer Research, 2017, 77, 7109-7119. 0.9 7 133 Optimizingsoj ethyl cellulose-ethanol delivery towards enabling ablation of cervical dysplasia. Scientific 3.3 7 134 Radiologic-pathologic analysis of increased ethanol localization and ablative extent achieved by ethyl 3.3 7 134 Radiologic-pathologic analysis of increased ethanol localization and ablative extent achieved by ethyl 3.3 7 136 A compact, cost-effective diffuse reflectance spectroscopic imaging system for quantitative tissue 0.8 6 136 A compact, cost-effective diffuse reflectance spectroscopic imaging system for quantitative tissue 0.8 6 136 Combining multiple contrasts for improving machine learning-based classification of cervical cancers with a low-cost point-of-care Pocket colposcope , 2020, 2020, 1148-1151. 6 137 Combining multiple contrasts for improving machine learning-based classification of cervical cancers with a low-cost point-of-care Pocket colposcope , 2020, 2020, 1148-1151. 5 138 Quantitative spectral reflectance imaging device for intraoperative breast tumor margin assessment. , 2009, 2009, 6554-6. 5 139 An Accessible Laparoscope for Surgery in Low- and Middle- Income Countries. Annals of Biomedical Pictores and Photobiology, 2007, 78, 462-469. 4 141 Custom annul	131	Correlation of breast tissue histology and optical signatures to improve margin assessment techniques. Journal of Biomedical Optics, 2016, 21, 066014.	2.6	7
133 Reports, 2021, 11, 16869. 3.3 7 134 Radiologic-pathologic analysis of increased ethanol localization and ablative extent achieved by ethyl 3.3 7 134 Cellulose. Scientific Reports, 2021, 11, 20700. 0.8 6 135 A compact, cost-effective diffuse reflectance spectroscopic imaging system for quantitative tissue absorption and scattering. Proceedings of SPIE, 2011,	132	Distinct Angiogenic Changes during Carcinogenesis Defined by Novel Label-Free Dark-Field Imaging in a Hamster Cheek Pouch Model. Cancer Research, 2017, 77, 7109-7119.	0.9	7
134 cellulose. Scientific Reports, 2021, 11, 20700. 3.3 7 135 Acompact, cost-effective diffuse reflectance spectroscopic imaging system for quantitative tissue absorption and scattering. Proceedings of SPIE, 2011,	133		3.3	7
135 absorption and scattering. Proceedings of SPIE, 2011, 0.8 6 136 Dark field optical imaging reveals vascular changes in an inducible hamster cheek pouch model during carcinogenesis. Biomedical Optics Express, 2016, 7, 3247. 2.9 6 137 Combining multiple contrasts for improving machine learning-based classification of cervical cancers with a low-cost point-of-care Pocket colposcope. , 2020, 2020, 1148-1151. 6 138 Quantitative spectral reflectance imaging device for intraoperative breast tumor margin assessment. , 2009, 2009, 6554-6. 5 139 An Accessible Laparoscope for Surgery in Low- and Middle- Income Countries. Annals of Biomedical Engineering, 2021, 49, 1657-1669. 2.5 5 140 Autofluorescence Spectroscopy of Normal and Malignant Human Breast Cell Lines¶. Photochemistry and Photobiology, 2007, 78, 462-469. 4 141 Custom annular photodetector arrays for breast cancer margin assessment using diffuse reflectance spectroscopy. , 2011, 0.8 4 142 Tissue quantification in photon-limited microendoscopy. Proceedings of SPIE, 2011, 0.8 4	134		3.3	7
138 carcinogenesis. Biomedical Optics Express, 2016, 7, 3247. 2.9 6 137 Combining multiple contrasts for improving machine learning-based classification of cervical cancers with a low-cost point-of-care Pocket colposcope. , 2020, 2020, 1148-1151. 6 138 Quantitative spectral reflectance imaging device for intraoperative breast tumor margin assessment. , 2009, 2009, 6554-6. 5 139 An Accessible Laparoscope for Surgery in Low- and Middle- Income Countries. Annals of Biomedical Engineering, 2021, 49, 1657-1669. 2.5 5 140 Autofluorescence Spectroscopy of Normal and Malignant Human Breast Cell Lines¶. Photochemistry and Photobiology, 2007, 78, 462-469. 2.5 4 141 Custom annular photodetector arrays for breast cancer margin assessment using diffuse reflectance spectroscopy. , 2011, , . 0.8 4 142 Tissue quantification in photon-limited microendoscopy. Proceedings of SPIE, 2011, , . 0.8 4	135		0.8	6
137 cancers with a low-cost point-of-care Pocket colposcope., 2020, 2020, 1148-1151. 0 138 Quantitative spectral reflectance imaging device for intraoperative breast tumor margin assessment., 2009, 2009, 6554-6. 5 139 An Accessible Laparoscope for Surgery in Low- and Middle- Income Countries. Annals of Biomedical Engineering, 2021, 49, 1657-1669. 2.5 5 140 Autofluorescence Spectroscopy of Normal and Malignant Human Breast Cell Lines¶. Photochemistry and Photobiology, 2007, 78, 462-469. 2.5 4 141 Custom annular photodetector arrays for breast cancer margin assessment using diffuse reflectance spectroscopy., 2011, ,. 0.8 4 142 Tissue quantification in photon-limited microendoscopy. Proceedings of SPIE, 2011, ,. 0.8 4	136	Dark field optical imaging reveals vascular changes in an inducible hamster cheek pouch model during carcinogenesis. Biomedical Optics Express, 2016, 7, 3247.	2.9	6
138 2009, 2009, 6554-6. 5 139 An Accessible Laparoscope for Surgery in Low- and Middle- Income Countries. Annals of Biomedical 2.5 5 140 Autofluorescence Spectroscopy of Normal and Malignant Human Breast Cell Lines¶. Photochemistry 2.5 4 141 Custom annular photodetector arrays for breast cancer margin assessment using diffuse reflectance 4 142 Tissue quantification in photon-limited microendoscopy. Proceedings of SPIE, 2011, , . 0.8 4 142 Spectroscopic diagnosis of cervical intraepithelial neoplasia (CIN) in vivo using laserâ€induced 0.8 4	137	Combining multiple contrasts for improving machine learning-based classification of cervical cancers with a low-cost point-of-care Pocket colposcope. , 2020, 2020, 1148-1151.		6
 Engineering, 2021, 49, 1657-1669. Autofluorescence Spectroscopy of Normal and Malignant Human Breast Cell Lines¶. Photochemistry and Photobiology, 2007, 78, 462-469. Custom annular photodetector arrays for breast cancer margin assessment using diffuse reflectance Custom annular photodetector arrays for breast cancer margin assessment using diffuse reflectance Tissue quantification in photon-limited microendoscopy. Proceedings of SPIE, 2011, , . Spectroscopic diagnosis of cervical intraepithelial neoplasia (CIN) in vivo using laserâ€induced 	138			5
140 and Photobiology, 2007, 78, 462-469. 2.3 4 141 Custom annular photodetector arrays for breast cancer margin assessment using diffuse reflectance spectroscopy., 2011, , . 4 142 Tissue quantification in photon-limited microendoscopy. Proceedings of SPIE, 2011, , . 0.8 4 148 Spectroscopic diagnosis of cervical intraepithelial neoplasia (CIN) in vivo using laserâ€induced 0.1 4	139		2.5	5
141 spectroscopy., 2011, , . 4 142 Tissue quantification in photon-limited microendoscopy. Proceedings of SPIE, 2011, , . 0.8 4 142 Spectroscopic diagnosis of cervical intraepithelial neoplasia (CIN) in vivo using laserâ€induced 0.8 4	140	Autofluorescence Spectroscopy of Normal and Malignant Human Breast Cell Lines¶. Photochemistry and Photobiology, 2007, 78, 462-469.	2.5	4
Spectroscopic diagnosis of cervical intraepithelial neoplasia (CIN) in vivo using laserâ€induced	141			4
	142	Tissue quantification in photon-limited microendoscopy. Proceedings of SPIE, 2011, , .	0.8	4
fluorescence spectra at multiple excitation wavlengths. Lasers in Surgery and Medicine, 1996, 19, 63-74.	143	Spectroscopic diagnosis of cervical intraepithelial neoplasia (CIN) in vivo using laserâ€induced fluorescence spectra at multiple excitation wavlengths. Lasers in Surgery and Medicine, 1996, 19, 63-74.	2.1	4

144 Diffuse reflectance spectral imaging for breast tumor margin assessment. , 2012, , .

#	Article	IF	CITATIONS
145	Understanding the sources of errors in ex vivo Hsp90 molecular imaging for rapid-on-site breast cancer diagnosis. Biomedical Optics Express, 2021, 12, 2299.	2.9	3
146	Imaging of 2-NBDG and TMRE reveals glucose uptake and mitochondrial membrane potential in dorsal window chamber models. , 2017, , .		3
147	Assessing effects of pressure on tumor and normal tissue physiology using an automated self-calibrated, pressure-sensing probe for diffuse reflectance spectroscopy. Journal of Biomedical Optics, 2018, 23, 1.	2.6	3
148	A Spectroscopic Technique to Simultaneously Characterize Fatty Acid Uptake, Mitochondrial Activity, Vascularity, and Oxygen Saturation for Longitudinal Studies In Vivo. Metabolites, 2022, 12, 369.	2.9	3
149	Optical spectroscopy vs. the surgical suite [cancer detection]. IEEE Circuits and Devices: the Magazine of Electronic and Photonic Systems, 1996, 12, 34-40.	0.4	2
150	Visualization of Morphological and Molecular Features Associated with Chronic Ischemia in Bioengineered Human Skin. Microscopy and Microanalysis, 2010, 16, 117-131.	0.4	2
151	Calibration schemes of a field-compatible optical spectroscopic system to quantify neovascular changes in the dysplastic cervix. , 2011, , .		2
152	Experimental validation of an inverse fluorescence Monte Carlo model to extract concentrations of metabolically relevant fluorophores from turbid phantoms and a murine tumor model. Journal of Biomedical Optics, 2012, 17, 078003.	2.6	2
153	Development and utilization of a novel cervical visualization tool, the Callascope, for home-based self-exams. Gynecologic Oncology, 2021, 162, S128-S129.	1.4	2
154	Longitudinal Monitoring of 4T1-Tumor Physiology in vivo with Doxorubicin Treatment via Diffuse Optical Spectroscopy. , 2008, , .		2
155	Policy Considerations to Promote Equitable Cervical Cancer Screening and Treatment in Peru. Annals of Global Health, 2021, 87, 116.	2.0	2
156	[18F]Fluoro-DCP, a first generation PET radiotracer for monitoring protein sulfenylation in vivo. Redox Biology, 2022, 49, 102218.	9.0	2
157	A scaling Monte Carlo method for diffuse reflectance computation from multi-layered media. , 2007, , .		1
158	Relationship Between Collagen Autofluorescence of the Human Cervix and Menopausal Status. Photochemistry and Photobiology, 2007, 77, 653-658.	2.5	1
159	A self-calibrating fiber optic probe for tissue optical spectroscopy. , 2008, , .		1
160	Using wide-field quantitative diffuse reflectance spectroscopy in combination with high-resolution imaging for margin assessment. Proceedings of SPIE, 2011, , .	0.8	1
161	Resetting the tumor microenvironment to favor anti-tumor immunity after local ablation Journal of Clinical Oncology, 2021, 39, 2561-2561.	1.6	1
162	Ethanol ablation reliably achieves an anti-metastatic response after modulating tumor acidity and regulatory T cells. Gynecologic Oncology, 2021, 162, S150.	1.4	1

#	Article	IF	CITATIONS
163	Optimizing fluorescently-tethered Hsp90 inhibitor dose for maximal specific uptake by breast tumors. , 2018, , .		1
164	In vivo Multiphoton Fluorescence Lifetime Imaging of Free and Protein-bound NADH in Normal and Pre-cancerous Epithelia. , 2006, , .		1
165	Optical Spectral Imaging For Breast Margin Assessment: A Comprehensive Assessment of Sources of Contrast. , 2012, , .		1
166	Hyperspectral Imaging of Glucose Uptake, Mitochondrial Membrane Potential, and Vascular Oxygenation Differentiates Breast Cancers with Distinct Metastatic Potential In Vivo. , 2016, , .		1
167	Leveraging Surface Hsp90 Expression for Rapid-on-site Breast Cancer Diagnostics. , 2020, , .		1
168	Detection of cervical precancer using optical spectroscopy (Extended Abstract). , 1996, , .		0
169	On-line monitoring of oxy- and deoxy-hemoglobin using near-infrared spectroscopic techniques. , 2001, , .		0
170	Noninvasive cerebral hemoglobin oxygenation quantification of fetal sheep under hypoxic stress in utero using frequency-domain diffuse optical two-layer model. , 2003, , .		0
171	Assessment of breast tumor margins via quantitative diffuse reflectance imaging. Proceedings of SPIE, 2010, , .	0.8	0
172	A custom wide-field spectral imager for breast cancer margin assessment. , 2011, , .		0
173	Rapid Determination of Tissue Hemoglobin Concentration and Oxygen Saturation of Head and Neck Cancers for Global Health Applications. , 2012, , .		0
174	Quantitative segmentation of fluorescence microscopy images of heterogeneous tissue: Approach for tuning algorithm parameters. , 2013, , .		0
175	Monitoring of cycling hypoxia and angiogenesis in FaDu head and neck tumors using a side-firing sensor. , 2013, , .		0
176	Optical monitoring of glucose demand and vascular delivery in a preclinical murine model. Proceedings of SPIE, 2014, , .	0.8	0
177	Special Section Guest Editorial: Light for Life: International Year of Light 2015. Journal of Biomedical Optics, 2015, 20, 061101.	2.6	0
178	Portable System for Wide-field, Sub-millimeter Functional Imaging of the Morphological Landscape of Breast Tumor Margins. , 2016, , .		0
179	Quantitative assessment of distant recurrence risk in early stage breast cancer using a nonlinear combination of pathological, clinical and imaging variables. Journal of Biophotonics, 2020, 13, e201960235.	2.3	0
180	A novel treatment for recurrent localized cervical cancer using point-of-care ethyl cellulose ethanol ablation with concurrent cytotoxic therapy Journal of Clinical Oncology, 2021, 39, e17507-e17507.	1.6	0

#	Article	IF	CITATIONS
181	Transabdominal Near-infrared Fetal Brain Oximetry. , 2004, , .		Ο
182	Monte Carlo based inverse model of diffuse reflectance for determination of UV-VIS optical properties and its application to breast cancer diagnosis. , 2004, , .		0
183	The use of a multi-separation probe for optical diagnosis of breast cancer. , 2004, , .		о
184	Angled probe design for scattering measurements from a small tissue volume. , 2006, , .		0
185	Monte Carlo Based Model of Fluorescence: Theory and Application to Breast Cancer Diagnosis. , 2006, , .		0
186	In vivo Fluorescence Spectroscopy during Breast Core Needle Biopsy. , 2006, , .		0
187	Physiologic, Metabolic, and Structural Alterations in Breast Cancer: Assessment via Optical Technologies. , 2006, , .		0
188	In Vivo Estimation of Total Hemoglobin Concentration and Hemoglobin Saturation in the Detection of Cervical Epithelial Pre-cancers. , 2007, , .		0
189	A Miniature Optical Device for Noninvasive, Fast Characterization of Tumor Pathology. , 2008, , .		Ο
190	Optical Biomarkers in Breast Cancer. , 2008, , .		0
191	Factors Influencing the Accuracy of Determining Tissue Physiology Quantitatively Using Optical Spectroscopy. , 2008, , .		Ο
192	In vivo quantification of tumor metabolic demand in preclinical models using optical spectroscopy. , 2012, , .		0
193	Optimization of Illumination Frequency and Preclinical Validation of a Wide-field Structured Illumination Microscope Designed for Imaging in situ Tumor Margins. , 2013, , .		0
194	Structured Illumination Fluorescence Imaging and Analysis for Identification of Residual Disease during Cancer Surgery. , 2014, , .		0
195	In vivo metabolic imaging reveals mitochondrial membrane potential reprogramming following Her2-targeted therapy and dormant disease. , 2020, , .		0
196	Editorial overview: Biomedical Engineering and Women's Health - Breaking new ground in gender and sex-specific research. Current Opinion in Biomedical Engineering, 2022, , 100392.	3.4	0